International Journal of Engineering

Journal Homepage: www.ije.ir

Seamless Transition in Grid-connected Microgrid System using Proportional Resonant Controller

V. Lavanya*, N. Senthil Kumar

School of Electrical Engineering, Vellore Institute of Technology, Chennai, Tamilnadu, India

P A P E R I N F O

Paper history:
Received 28 December 2019
Received in revised form 14 July 2020
Accepted 07 August 2020

Keywords:
Grid-connected
Microgrid
Seamless Transition
Distributed Generation
Indirect Current Control
Proportional Resonant

A B S T R A C T

In this paper, the design of an inverter control structure based on the Proportional Resonant (PR) controller is dealt with in detail for attaining smooth transitions between the operating modes of a grid-connected microgrid system. The control strategy applied for the inverter is cascaded three-loop control viz., the grid current, voltage across the load, and the inverter output current loops. The inverter control is mainly focused to retain the voltage magnitude within the prescribed set limits and to have a good quality of the voltage across the load under all the modes of operation. A proportional resonant controller is designed by considering the transients and stability criteria into account under varying modes of operation. The design procedure of the Proportional resonant controller is given in detail. The three-phase grid-connected microgrid system considered under study is simulated in MATLAB/Simulink environment to operate under islanding condition as well as grid-connected condition and also changing modes from islanding to grid connected and vice versa. The simulation results are presented under various modes of operation to validate the controller design for a smooth transition between the modes of operation.

***doi**: 10.5829/ije.2020.33.10a.13*

1. INTRODUCTION

Renewable energy sources (RES) based power generation becomes a more and more viable solution for meeting the increase in the energy demand of today's electricity market. The power electronic interfaces such as boost converters, inverters are used as intermediate structures to connect the Distributed Energy Resources (DER) like Solar PV, Wind, fuel cells, etc., to the grid. A microgrid (MG) is one that comprises a low voltage (LV) or medium voltage (MV) group of DERs which are controlled locally. A MG may look like a single power producer or a load [1-4] when considered from the grid's perspective. A MG can operate in conjunction with the utility to feed in a fraction of the total load while operating in grid connected condition and feeds critical loads in islanded mode i.e. when the utility grid is lost during any abnormal conditions [5]. The islanding state can be detected by islanding detection methods [6]. Under islanded mode, the microgrid feeds the critical loads while preserving the load voltage as well as the frequency within the limits, hence improving the reliability of the system [7]. The inverter which is between the sources and the loads and its control plays a vital role in the environment of a distributed generation when dealing with voltage quality and hence power quality.

The three-phase inverter of the DG system should be controlled to be operated under both grid-connected and islanded mode. The design of the inverter control is to be focused on the operating modes of the MG system and also it needs to take care of the smooth transition among the different states of microgrid operation like grid on and grid off, to reduce the voltage fluctuations across the critical loads when islanded and any sort of sudden changes in the current that is fed to the grid in grid-connected mode [8].

There are different control structures proposed in the literature for achieving fluctuations free transfer between the operating modes [9-21] to retain the power quality

*Corresponding Author Institutional Email: *lavanya.v@vit.ac.in* (V. Lavanya)

Please cite this article as: V. Lavanya and N. Senthil Kumar, Seamless Transition in Grid connected Microgrid System using Proportional Resonant Controller, International Journal of Engineering (IJE), IJE TRANSACTIONS A: Basics Vol. 33, No. 10, (October 2020) 1951-1958

during the transfers. Conventionally, an inverter that is connected to the grid is controlled as PQ control to feed/take power to/from the utility, and when the inverter gets disconnected from the grid V/f control is used for the maintenance of voltage across the load. When there is a need for switching between the modes, then switching between the controllers has to take place, which may lead to large transients and further may lead to system collapse. The inverter, when being operated as utility connected, is to be treated as a current source and when it gets disconnected from the utility, it is operated as a voltage source [9-11]. A droop characteristic adjustment based control scheme has been proposed in [12]. An inverter control technique with an inner voltage control loop and outer current control loop has been discussed in [13] for seamless transfer in microgrids. In [14], the output current of the inverter is controlled to regulate the current fed to the grid, at the same time the load voltage is maintained without any variation.

Indirect current control with Proportional Integral (PI) controller, which is based on synchronous reference (d–q) frame, has been used for seamless transfer [15-23], in which case the grid current is indirectly controlled with the help of capacitor voltage control. To improve the dynamics, the damping is introduced with the inverter side inductor current control loop or the filter capacitor voltage control loop. Under islanded mode, limiters are placed to limit the set value of the voltage for the inner voltage loop. Although seamless transitions between the modes have been achieved, the quality of the voltage waveform is a little bit affected as the voltage set value is limited with the threshold value. Proportional resonant (PR) control in a stationary reference frame has been proposed for transient free mode transitions [24-26].

In this paper, indirect current control based seamless transition is discussed in detail. Also, the design procedure of the Proportional resonant controller for the cascaded three-loop inverter control structure is presented in detail for achieving the smooth transition between the operating modes of a microgrid system.

2. MODELING AND DESIGN OF GRID CONNECTED INVERTER SYSTEM

2. 1. Modeling of the Power Stage The power stage of a three-phase inverter system is modeled based on a stationary reference frame and is shown in Figure 1.

The input voltage of the inverter is considered as a constant voltage and therefore, the control structure of the source side converter like a DC-DC boost converter [27, 28] that may be required to increase and regulate the dc-link voltage in a PV based system is not discussed in this paper.

After the inverter, the output voltage is filtered with the help of a passive filter of type, inductor-capacitor-

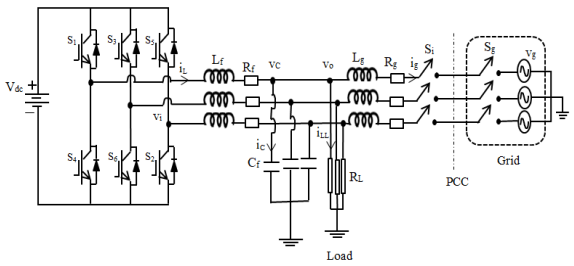

Figure 1. Power stage of a grid-connected inverter system

inductor (LCL) filter and is then connected to the utility grid. The critical/local loads are connected across the filter capacitor. The switches on both, grid side and the inverter side are turned on while operating in grid-connected condition and the grid side switch is turned off under faulty conditions leading the system to operate under islanded mode.

The basic mathematical equations governing the grid-connected inverter system with an LCL filter are given by Equations (1) and (2).

$$\frac{V_{dc}}{2}.\begin{pmatrix} d_a \\ d_b \\ d_c \end{pmatrix} = L_f.\frac{d}{dt}\begin{pmatrix} i_{La} \\ i_{Lb} \\ i_{Lc} \end{pmatrix} + R_f.\begin{pmatrix} i_{La} \\ i_{Lb} \\ i_{Lc} \end{pmatrix} + \begin{pmatrix} v_{ca} \\ v_{cb} \\ v_{cc} \end{pmatrix} \quad (1)$$

$$\begin{pmatrix} i_{La} \\ i_{Lb} \\ i_{Lc} \end{pmatrix} = C_f.\frac{d}{dt}\begin{pmatrix} v_{ca} \\ v_{cb} \\ v_{cc} \end{pmatrix} + \begin{pmatrix} i_{LLa} \\ i_{LLb} \\ i_{LLc} \end{pmatrix} + \begin{pmatrix} i_{ga} \\ i_{gb} \\ i_{gc} \end{pmatrix} \quad (2)$$

These a-b-c reference frame quantities are transformed into stationary reference frame parameters with the help of Clarke's transformation and the controllers are designed in the α-β reference frame.

2. 2. Design of LCL Filter The specification of the parameters used in the DG system considered is given in Table 1.

TABLE 1. Simulation Parameters of the MG System

Parameters	Symbol	Value
DC link voltage	V_{dc}	700 V
Filter inductor	L_f	3.11 mH
Filter capacitor	C_f	10 µF
Switching frequency	f_s	20 kHz
Grid side inductor	L_g	3.11 mH
Grid frequency	f_g	50 Hz
Grid voltage	V_g	220 V(rms)
Rated power of DG	P_{DG}	10 kW
Power rating of Load	P_L	5 kW

The filter and the control loop parameters are designed based on the DG specifications. As the output from the DG system is to be connected to the load/grid via a power electronics interface, harmonics gets into the system parameters. Hence, the inverter output is to be filtered to remove the harmonics present in it. The passive filter of type LCL is being used to filter out the harmonics and is designed to have the harmonics within the limits for the current as per standard IEEE Standard 519 -2014 [29].

The base impedance and the base capacitance values are calculated based on the Equations (3) and (4).

$$Z_{base} = \frac{V_{L-L}^2}{P_{nominal}} \quad (3)$$

$$C_{base} = \frac{1}{\omega_g Z_{base}} \quad (4)$$

The filter capacitance is found out from (5) by considering the variation seen by the grid as 5%.

$$C_f = 0.05 * C_{base} \quad (5)$$

The current ripple is calculated based on (6) by considering the ripple present as 10% of the rated current.

$$\Delta I_{max} = 10\% * I_{max} \quad (6)$$

where I_{max} is given by (7).

$$I_{max} = \frac{\sqrt{2} P_{nominal}}{3 V_{ph}} \quad (7)$$

The filter inductors, L_f in the inverter side and L_g in the grid side are calculated based on the Equations (8) and (9),

$$L_f = \frac{V_{dc}}{16 f_s \Delta I_{max}} \quad (8)$$

$$L_g = r L_f \quad (9)$$

where V_{dc} is the dc link voltage, f_s is the switching frequency of the inverter switches and r is the ratio between inverter side inductor and grid side inductor and the value of r is be considered based on the nominal grid impedance and the resonant frequency from the transfer function of the filter. The resonant frequency is specified by (10) and the constraint is given by (11).

$$\omega_{res} = \sqrt{\frac{L_f + L_g}{L_f L_g C_f}} \quad (10)$$

$$10 f_g < f_{res} < 0.5 f_s \quad (11)$$

2. 3. Controller Design The basic control diagram representation of the indirect current control scheme based on the PR controller is shown in Figure 2. The cascaded three-loop control structure consists of an outer grid current control loop, inner capacitor voltage control loop, and an innermost inductor current control loop. The cascaded loops are designed with proper bandwidth

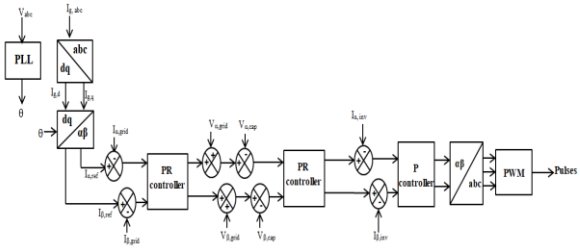

Figure 2. Indirect current control structure based on the PR controller

selection. The design of the inner voltage control loop is done to get the voltage across the load to be maintained as per the requirement in all the operating modes.

2. 3. 1. Design of Innermost Inductor Current Control Loop The innermost inductor current controller structure is shown in Figure 3.

From Figure 3, the plant transfer function is given by (12) and the open-loop transfer function of the current control loop is given by (13).

$$G(s) = \frac{I_L(s)}{V_i(s)} = \frac{s C_f}{s^2 L_f C_f + 1} \quad (12)$$

$$G_{OL,IC}(s) = \frac{K_{PWM} * k_{p1} * s C_f}{s^2 L_f C_f + 1} \quad (13)$$

where k_{p1} is the proportional controller gain and K_{PWM} is the gain of the converter and is considered as 1 for simplicity.

The closed-loop transfer function of the inner current controller is given by (14).

$$\frac{I_L(s)}{I_{L,ref}(s)} = \frac{s k_{p1} k_{PWM} C_f}{s^2 L_f C_f + s k_{p1} k_{PWM} C_f + 1} \quad (14)$$

The root locus plot is used to design the controller gains and is shown in Figure 4. From Figure 4, the proportional gain of the current controller is chosen to be 35.3 as the oscillations get damped out when the gain k_{p1} is ≥ 35.3.

2. 3. 2. Design of the Capacitor Voltage Control Loop The capacitor voltage control loop structure is shown in Figure 5. The root locus plot is used to find the values of k_p and k_i of the PR controller. Figure 6 shows the root locus plot of the system which is used for finding the value of k_p with k_i=0. The value of k_p is found to be 0.0285 for a damping ratio of 0.707.

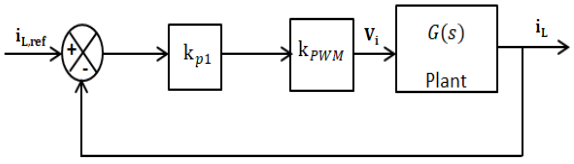

Figure 3. Innermost inductor current controller

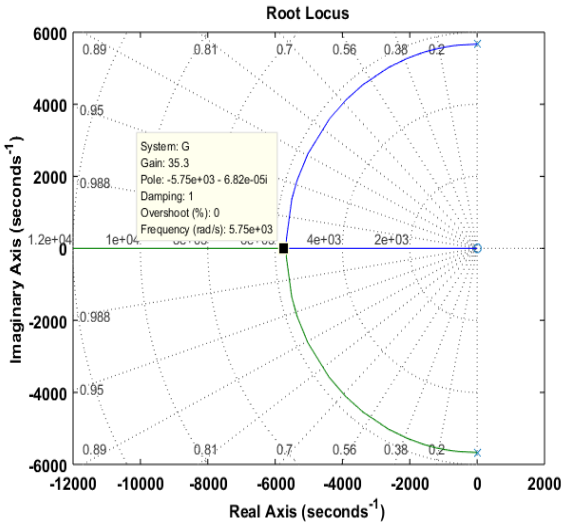

Figure 4. Root locus plot of the innermost current control loop

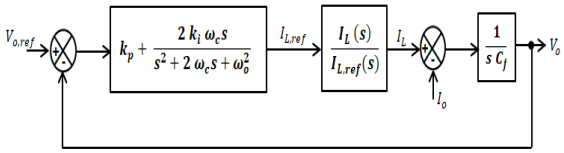

Figure 5. Capacitor voltage control loop structure

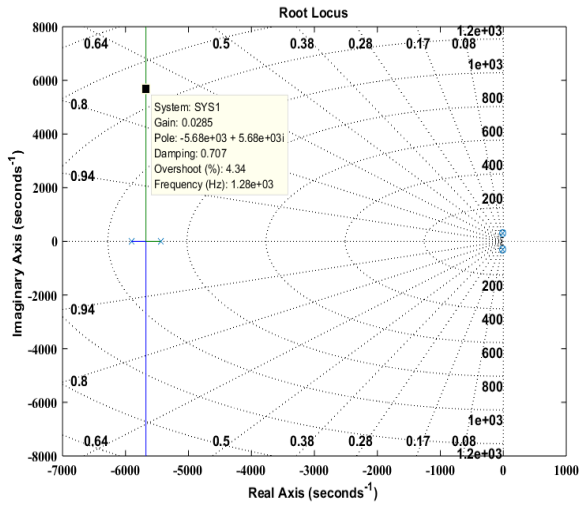

Figure 6. Root locus plot of voltage controller considering k_i=0

The closed-loop transfer function of the voltage control loop is given by (15).

$$\frac{V_o(s)}{V_{o,ref}(s)} = \frac{\left(k_p + \frac{2 k_i \omega_c s}{s^2 + 2 \omega_c s + \omega_o^2}\right) * \frac{I_L(s)}{I_{L,ref}(s)} * \frac{1}{s C}}{1 + \left(k_p + \frac{2 k_i \omega_c s}{s^2 + 2 \omega_c s + \omega_o^2}\right) * \frac{I_L(s)}{I_{L,ref}(s)} * \frac{1}{s C}} \quad (15)$$

Figure 7 shows the root locus plot of the voltage control loop with k_p= 0. The value of k_i is found to be 4.86 for a damping ratio of 0.707. The bode diagram of the open-loop transfer function (OLTF) of PR based voltage control loop with k_p=0.0285 and k_i =2.43 is shown in Figure 8. The gain at the fundamental frequency is 38.7 dB and the phase margin of the controller is 118.3°.

2. 3. 3. Design of the outer Grid Current Control Loop The outer grid current control loop structure is shown in Figure 9. The parameters of PR based current controller are found out to be $k_{p,1}$=6, and $k_{i,1}$=25 by using the same procedure as described above. Figure 10 shows the bode diagram of the OLTF of the grid current control, which gives the large gain at the fundamental frequency of 50 Hz and the phase margin of 61°.

The root locus plot and the bode diagram of the closed-loop transfer function (CLTF) of the overall system are shown in Figures 11 and 12.

3. SIMULATION RESULTS AND DISCUSSION

The system described in Figure 1 is simulated in MATLAB / Simulink environment. The parameters used for simulation studies are specified in Table 1. The

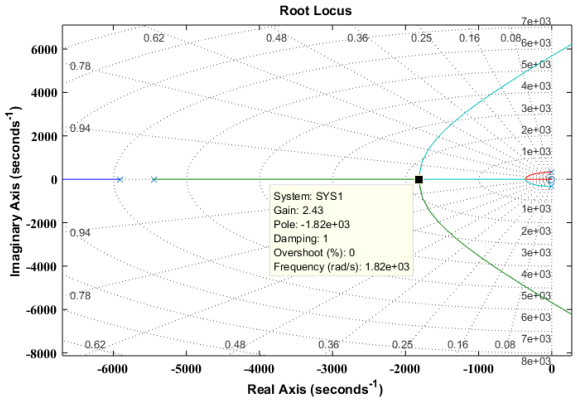

Figure 7. Root locus plot of voltage controller considering k_p=0

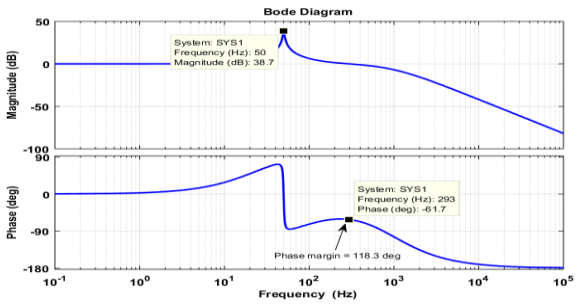

Figure 8. Bode diagram of OLTF of the Voltage controller

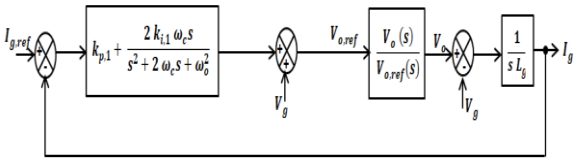

Figure 9. Outer grid current control loop structure

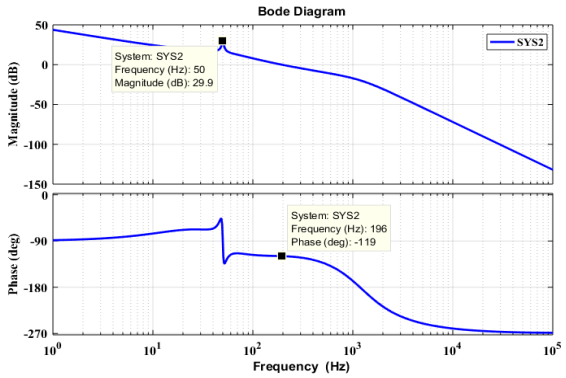

Figure 10. Bode diagram of OLTF of the grid current controller

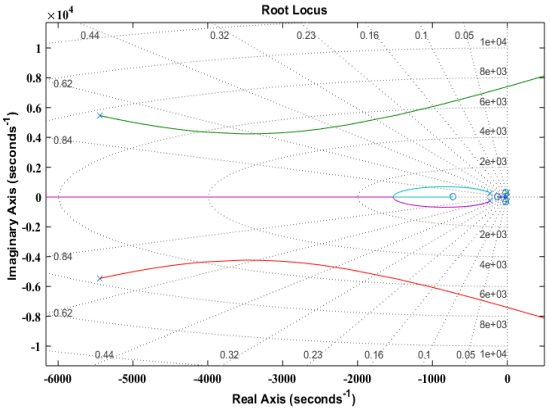

Figure 11. Root locus plot of the overall system

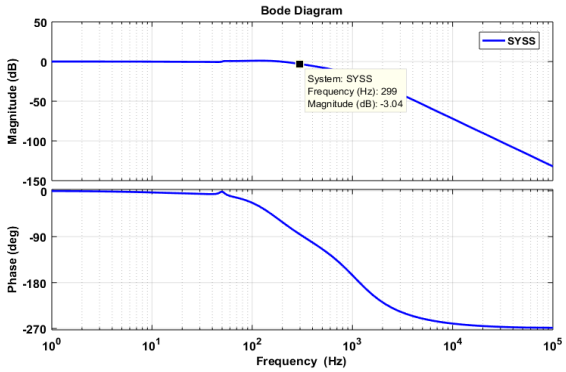

Figure 12. Bode diagram of the CLTF of grid current controller

system is first considered to be connected with the utility, feeding the local load as well as the grid. Simulation studies considering intentional and unintentional islanding have been carried out and the results are presented in this section.

3. 1. Intentional Islanding and Seamless Transfer to Grid Connected Mode Initially, the system is considered to be of grid-connected mode and is moved to islanded mode intentionally and then brought back to the grid-connected mode again. The DG system is in grid-connected mode from 0 – 0.32s and at 0.32s, both the switches 'S_g' and 'S_i' are opened and the system is moving to islanded mode. The system is feeding the load with the demanded power without any interruption. Both the switches are closed at 0.5s after the confirmation of synchronization of MG voltage with that of the utility and hence the DG system is reconnected to the utility at 0.5s. The waveforms of the voltage at the grid side and current fed to the grid under different operating conditions are shown in Figures 13-15.

The grid current falls to zero when moving to islanded mode, which is presented in Figure 14 and the grid current increases to the specified value (10A peak) within 2 cycles i.e., 40ms, immediately after the synchronization process is done, which is shown in Figure 15. The load parameters under different operating conditions are shown in Figures 16 and 17. At the time of moving to

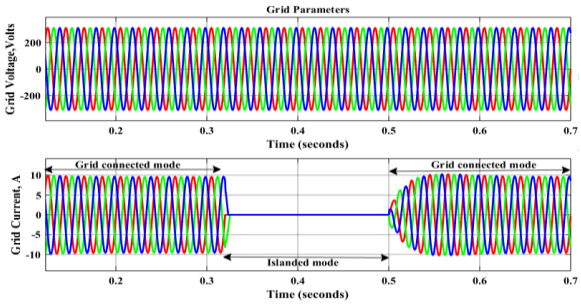

Figure 13. Voltage and Current waveforms at the grid side

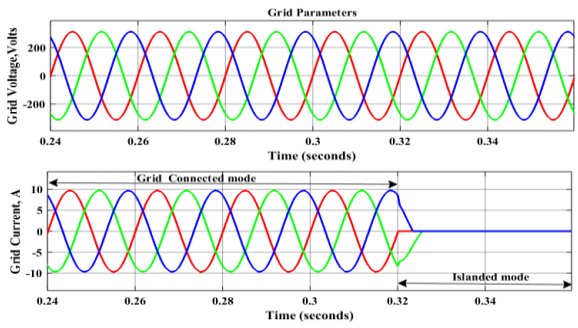

Figure 14. Grid voltage and grid current waveforms when mode changes from grid-connected to islanded mode

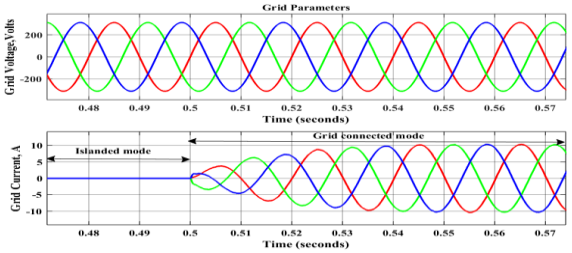

Figure 15. Grid voltage and grid current waveforms when mode changes from islanded to grid-connected mode

islanded mode i.e., at 0.32s, when the switch at the grid side opens, transient which occurs in the load parameters are damped and steady-state is reached within 20ms and the voltage across the load remains almost at the required steady value of about 220 V (rms) and the current is of 7.57 A (rms). The d-q components of the voltage across the load are shown in Figure 18 to show the voltage almost remains the same throughout the operating time. The power consumed by the load is shown in Figure 19.

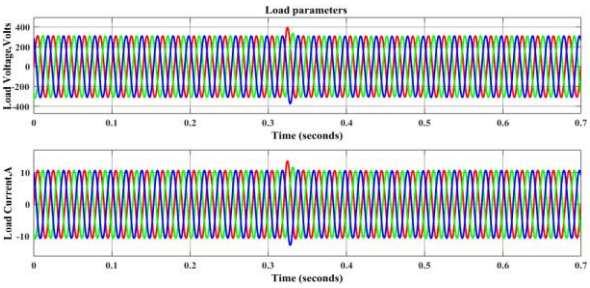

Figure 16. Load voltage and load current under different operating conditions

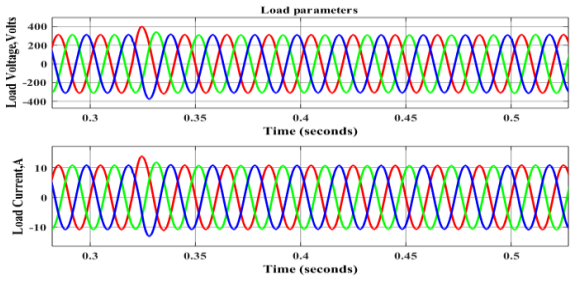

Figure 17. Load voltage and load current while moving to islanding mode and the grid-connected mode

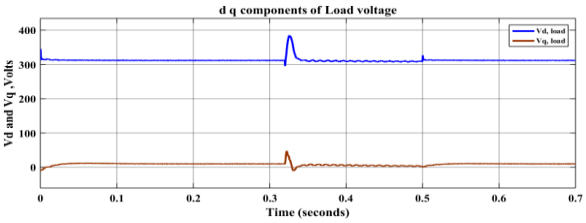

Figure 18. d q components of the load voltage

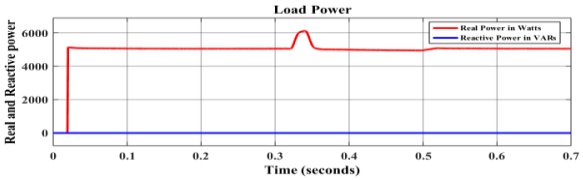

Figure 19. Real and reactive power consumed by the load

3. 2. Unintentional islanding and Seamless Transfer to Grid-connected Mode The system is initially considered to be operating in the grid-connected mode. A three-phase fault is simulated at 0.32s and the switch 'S_g' at the grid side is opened at 0.32s immediately after the occurrence of the fault. The switch 'S_i' in the inverter side is opened at 0.35 s after detecting the islanding condition. The duration between 0.32 s and 0.35s is called a Pre-islanded condition where the terminal voltage is slightly higher than the prescribed limit which is due to the occurrence of the disturbance. Then as the switch 'S_i' gets opened, the system enters into the islanded mode and the load is fed with the desired voltage and frequency without any distortion. After the clearance of the fault, the switch 'S_g' is closed at 0.55 s and the grid is restored. The DG can be connected to the grid only after the synchronization of the voltage at the DG with that of the grid. Hence after the synchronization process, the switch 'S_i' is closed at 0.7 s. The grid current reference is changed to the set value at 0.75 s and till then it remains zero. The current fed into the grid gradually increases and reaches the set value at 0.78s without any transients in the voltage as well in the current waveform.

The voltage and the current waveform at the grid side during the changeover of modes are shown in Figure 20 and Figure 21. The load voltage and load current waveforms are shown in Figure 22. Thus seamless transition between the modes of operation is achieved successfully with the help of an Indirect current control strategy using Proportional resonant controllers.

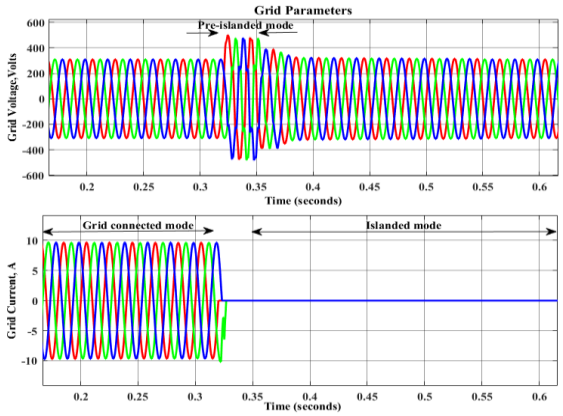

Figure 20. Grid voltage and grid current waveforms–grid-connected mode to islanded mode under unintentional islanding

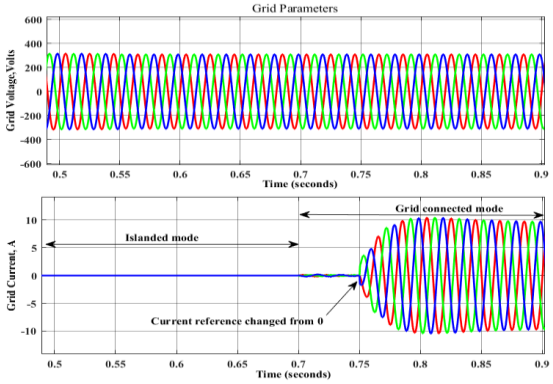

Figure 21. Grid voltage and grid current waveforms – islanded mode to grid-connected mode under unintentional islanding

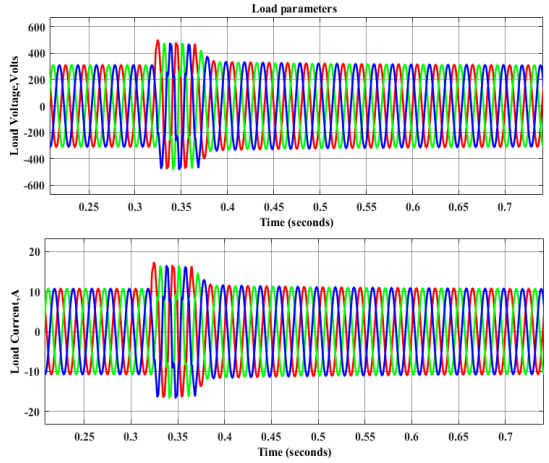

Figure 22. Load voltage and load current waveforms from the islanding mode to grid-connected mode

4. CONCLUSION

A three-phase grid-connected microgrid system has been designed and simulation studies have been carried out in MATLAB / Simulink environment. The proportional resonant controller-based indirect current control strategy has been designed for achieving the seamless transfer between the operating modes of a microgrid. The system considered is simulated in MATLAB/Simulink environment, under islanded and grid-connected modes of operation and the results are presented. Simulation studies have been carried out under intentional islanding and unintentional islanding conditions. The results validate the controller design. The PR based controller for the voltage source inverter works efficiently and effectively. Thus, the seamless transfer between the modes of operation with a very minimal transient period has been attained and the steady-state is reached within 0.04s after the closure or opening of the switches for changing of modes of operation based on the utility conditions.

5. REFERENCES

1. Chowdhury, S., Chowdhury, S. and Crossley, P., "Microgrids and active distribution networks (energy engineering)", Published by The Institution of Engineering and Technology, (2009),
2. Driesen, J. and Katiraei, F., "Design for distributed energy resources", ***IEEE Power and Energy Magazine***, Vol. 6, No. 3, (2008), 30-40. DOI:10.1109/MPE.2008.918703
3. Hatziargyriou, N., Asano, H., Iravani, R. and Marnay, C., "Microgrids", ***IEEE Power and Energy Magazine***, Vol. 5, No. 4, (2007), 78-94. DOI: 10.1109/MPAE.2007.376583
4. Lasseter, R.H., "Microgrids", in 2002 IEEE Power Engineering Society Winter Meeting. Conference Proceedings (Cat. No. 02CH37309), IEEE. Vol. 1, 305-308. DOI.10.1109/PESW.2002.985003
5. Olivares, D.E., Mehrizi-Sani, A., Etemadi, A.H., Cañizares, C.A., Iravani, R., Kazerani, M., Hajimiragha, A.H., Gomis-Bellmunt, O., Saeedifard, M. and Palma-Behnke, R., "Trends in microgrid control", ***IEEE Transactions on Smart Grid***, Vol. 5, No. 4, (2014), 1905-1919. DOI:10.1109/TSG.2013.2295514
6. Gholami, M., "Islanding detection method of distributed generation based on wavenet", ***International Journal of Engineering***, Vol. 32, No. 2, (2019), 242-248. DOI: 10.5829/ije.2019.32.02b.09
7. "IEEE Standard for Interconnection and Interoperability of Distributed Energy Resources with Associated Electric Power Systems Interfaces," in IEEE Std 1547-2018 (Revision of IEEE Std 1547-2003) ,1-138, 2018, doi: 10.1109/IEEESTD.2018.8332112.
8. Carrasco, J.M., Franquelo, L.G., Bialasiewicz, J.T., Galván, E., PortilloGuisado, R.C., Prats, M.M., León, J.I. and Moreno-Alfonso, N., "Power-electronic systems for the grid integration of renewable energy sources: A survey", ***IEEE Transactions on Industrial Electronics***, Vol. 53, No. 4, (2006), 1002-1016. DOI: 10.1109/TIE.2006.878356
9. Balaguer, I.J., Lei, Q., Yang, S., Supatti, U. and Peng, F.Z., "Control for grid-connected and intentional islanding operations of distributed power generation", ***IEEE Transactions on Industrial Electronics***, Vol. 58, No. 1, (2010), 147-157. DOI: 10.1109/TIE.2010.2049709
10. Gaonkar, D., Pillai, G. and Patel, R., "Seamless transfer of microturbine generation system operation between grid-connected and islanding modes", ***Electric Power Components and Systems***, Vol. 37, No. 2, (2009), 174-188. DOI:10.1080/15325000802388815
11. Ahmed, I., Longting, S. and Xin, C., "A novel control scheme for microgrid inverters seamless transferring between grid-connected and islanding mode", in 2017 China International Electrical and Energy Conference (CIEEC), IEEE. 75-80. DOI: 10.1109/CIEEC.2017.8388423
12. Jia, Y., Liu, D. and Liu, J., "A novel seamless transfer method for a microgrid based on droop characteristic adjustment", in Proceedings of The 7th International Power Electronics and Motion Control Conference, IEEE. Vol. 1, 362-367. DOI: 10.1109/IPEMC.2012.6258878
13. Shen, G., Xu, D. and Yuan, X., "A novel seamless transfer control strategy based on voltage amplitude regulation for utility-interconnected fuel cell inverters with an lcl-filter", in 2006 37th IEEE Power Electronics Specialists Conference, IEEE. 1-6. DOI: 10.1109/pesc.2006.1712073
14. Yanjie, W. and Guopeng, Z., "An output current based seamless transfer control strategy for three-phase converter with energy storage in micro-grid", International Conference on Renewable Power Generation (RPG 2015), Beijing, China**,** (2015) 1-6. DOI: 10.1049/cp.2015.0310.

15. Gao, F. and Iravani, M.R., "A control strategy for a distributed generation unit in grid-connected and autonomous modes of operation", ***IEEE Transactions on Power Delivery***, Vol. 23, No. 2, (2008), 850-859. DOI:10.1109/TPWRD.2007.915950
16. Hu, S.-H., Kuo, C.-Y., Lee, T.-L. and Guerrero, J.M., "Droop-controlled inverters with seamless transition between islanding and grid-connected operations", in 2011 IEEE Energy Conversion Congress and Exposition, IEEE. 2196-2201. DOI: 10.1109/ECCE.2011.6064059
17. Yu, T., Choi, S. and Kim, H., "Indirect current control algorithm for utility interactive inverters for seamless transfer", in 2006 37th IEEE Power Electronics Specialists Conference, IEEE. 1-6. DOI**:** 10.1109/pesc.2006.1712024
18. Kim, H., Yu, T. and Choi, S., "Indirect current control algorithm for utility interactive inverters in distributed generation systems", ***IEEE Transactions on Power Electronics***, Vol. 23, No. 3, (2008), 1342-1347. DOI: 10.1109/TPEL.2008.920879
19. Kwon, J., Yoon, S. and Choi, S., "Indirect current control for seamless transfer of three-phase utility interactive inverters", ***IEEE Transactions on Power Electronics***, Vol. 27, No. 2, (2011), 773-781. DOI: 10.1109/APEC.2011.5744661
20. Liu, Z., Liu, J. and Zhao, Y., "A unified control strategy for three-phase inverter in distributed generation", ***IEEE Transactions on Power Electronics***, Vol. 29, No. 3, (2013), 1176-1191. DOI: 10.1109/TPEL.2013.2262078
21. Liu, Z. and Liu, J., "Indirect current control based seamless transfer of three-phase inverter in distributed generation", ***IEEE Transactions on Power Electronics***, Vol. 29, No. 7, (2013), 3368-3383. DOI**:** 10.1109/TPEL.2013.2282319
22. Mohamed, Y.A.-R.I. and Radwan, A.A., "Hierarchical control system for robust microgrid operation and seamless mode transfer in active distribution systems", ***IEEE Transactions on Smart Grid***, Vol. 2, No. 2, (2011), 352-362. DOI: 10.1109/TSG.2011.2136362
23. Lavanya, V. and Kumar, N.S., "Control strategies for seamless transfer between the grid-connected and islanded modes of a microgrid system", ***International Journal of Electrical & Computer Engineering***, Vol. 10, No. 5, (2020), 4490-4506 DOI:10.11591/ijece.v10i5.pp4490-4506
24. Lim, K. and Choi, J., "Pr based indirect current control for seamless transfer of grid-connected inverter", in 2016 IEEE 8th International Power Electronics and Motion Control Conference (IPEMC-ECCE Asia), IEEE. 3749-3755. DOI: 10.1109/IPEMC.2016.7512895
25. Lim, K. and Choi, J., "Seamless grid synchronization of a proportional+ resonant control-based voltage controller considering non-linear loads under islanded mode", ***Energies***, Vol. 10, No. 10, (2017), 1514. DOI: 10.3390/en10101514
26. Lim, K., Song, I., Choi, J., Yoo, H.-J. and Kim, H.-M., "Seamless mode transfer of utility interactive inverters based on indirect current control", ***Journal of Power Electronics***, Vol. 19, No. 1, (2019), 254-264. DOI:10.6113/JPE.2019.19.1.254
27. Sagar, G. and Debela, T., "Implementation of optimal load balancing strategy for hybrid energy management system in dc/ac microgrid with pv and battery storage", ***International Journal of Engineering***, Vol. 32, No. 10, (2019), 1437-1445. DOI : 10.5829/ije.2019.32.10a.13
28. Gholizade-Narm, H., "A novel control strategy for a single-phase grid-connected power injection system", ***International Journal of Engineering***, Vol. 27, No. 12, (2014), 1841-1849. DOI:10.5829/idosi.ije.2014.27.12c.06
29. "IEEE Recommended Practice and Requirements for Harmonic Control in Electric Power Systems," in IEEE Std 519-2014 (Revision of IEEE Std 519-1992) , pp.1-29, 11 June 2014, doi: 10.1109/IEEESTD.2014.6826459.

Persian Abstract

چکیده

این مقاله به طراحی ساختار کنترل اینورتر مبتنی بر کنترلر متناسب با رزونانس (PR) برای دستیابی به انتقالهای صاف بین حالتهای عملیاتی یک سیستم میکروگرید متصل به شبکه پرداخته است. استراتژی کنترلی که برای اینورتر استفاده می شود عبارتست از کنترل سه حلقه آبشار ، جریان شبکه ، ولتاژ در طول بار و حلقه های جریان خروجی اینورتر. کنترل اینورتر عمدتاً برای حفظ مقدار ولتاژ در محدوده تعیین شده تعیین شده و داشتن کیفیت مناسب ولتاژ در طول بار تحت همه حالت های کار متمرکز است. یک کنترل کننده رزونانس متناسب با در نظر گرفتن معیارهای گذرا و پایداری در نظر گرفته شده در حالت های مختلف عملکرد طراحی شده است. روش طراحی کنترلر رزونانس متناسب با جزئیات ارائه شده است. سیستم میکروگرید متصل به شبکه سه فاز که مورد بررسی قرار گرفته است در محیط MATLAB / Simulink شبیه سازی شده است تا در شرایط جزیره ای و همچنین در شرایط اتصال به شبکه و همچنین تغییر حالت از جزیره به شبکه به شبکه متصل شده و برعکس. نتایج شبیه سازی تحت حالت های مختلف عملیاتی برای تأیید اعتبار طرح کنترل برای انتقال صاف بین حالت های عملکرد ارائه شده است.